Physicochem. Probl. Miner. Process., 62(4), 2026, 231237

http://www.journalssystem.com/ppmp

Physicochemical Problems of Mineral Processing

ISSN 1643-1049

Solution chemistry regulated foam behavior of sodium oleate and cetyl phosphate collectors: Mechanistic insights into magnesite flotation

Dongsheng He [1,2], Changming Xu [2], Yuan Tang [1,2], Fangyuan Li [2], Yanhong Fu [2], Zhili Li [1,2], Jiayu Ma [1]

[1] State Key Laboratory of Green and Efficient Development of Phosphorus Resources, Wuhan Institute of Technology, Wuhan 430074, China

[2] School of Resources and Safety Engineering, Wuhan Institute of Technology, Wuhan 430073, China

Corresponding author: yuan.tang@wit.edu.cn (Yuan Tang)

Abstract: This study systematically elucidates the distinct responses of two representative anionic collectors—sodium oleate (NaOl) and cetyl phosphate (CP)—to variations in pH and dissolved Ca^{2+}/Mg^{2+} concentrations. Dynamic foam analysis combined with surface tension measurements demonstrated that both collectors exhibited optimal yet fundamentally different pH-dependent foaming behaviors. CP generated highly stable foam under near-neutral conditions (pH ≈ 8), whereas severe foam destabilization occurred above pH 10 owing to enhanced electrostatic repulsion between fully ionized phosphate headgroups. In contrast, NaOl maintained excellent foam stability under alkaline conditions but lost foaming ability below pH 7.7 due to protonation of the carboxylate groups. The presence of divalent cations exerted pronounced detrimental effects, with significant ion-specific and collector-dependent characteristics. CP foamability was almost completely suppressed by trace Ca^{2+} concentrations as low as 1 ppm, whereas NaOl maintains favourable foaming performance at Ca^{2+} levels up to 10 ppm, which is likely associated with electrical double-layer compression. Low Mg^{2+} concentrations (≤5 ppm) slightly enhanced CP foam stability, whereas higher concentrations (≥10 ppm) significantly deteriorated the foam properties of both collectors. Compared with Mg^{2+}, Ca^{2+} exhibited a substantially stronger destabilizing effect, this difference can be tentatively attributed to the relatively lower hydration energy of Ca^{2+} as well as its comparatively higher tendency to form complexes with anionic surfactant headgroups. These findings provide important mechanistic insights into how solution chemistry regulates collector foam behavior in magnesite flotation systems. Future investigations combining dynamic foam analysis with batch flotation tests are required to quantitatively establish the relationship between bubble properties and flotation performance.

Keywords: dynamic foam analysis, froth flotation, solution chemistry, magnesite, cetyl phosphate

1. Introduction

Froth stability plays a critical role in mineral flotation because it directly governs bubble–particle transport, froth drainage behavior, and separation selectivity (Bournival et al., 2017; Xing et al., 2017; wang et al., 2020). However, flotation froths are thermodynamically unstable systems that continuously undergo liquid drainage, bubble coalescence, and film rupture during their evolution (Goncharik et al., 2013; Pan et al., 2022). The dynamic stability of flotation foam is therefore highly sensitive to interfacial physicochemical conditions, particularly the adsorption behavior and interfacial organization of surfactant molecules (Fukuoka et al., 2016; Moreno and Silva., 2021). Excessively unstable froths lead to premature bubble collapse and particle detachment, whereas overly persistent froths may hinder drainage and increase gangue entrainment, thereby reducing concentrate grade and process selectivity (Bhondayi C., 2020; Zhang et al., 2020). Consequently, understanding the factors governing foam stability is essential for optimizing flotation performance.

DOI: 10.37190/ppmp/231237

Among the various influencing factors, solution chemistry has been recognized as one of the most important regulators of flotation foam behavior. Previous studies have demonstrated that pH, ionic composition, and dissolved multivalent ions strongly influence surfactant dissociation, interfacial tension, and bubble coalescence processes (Pugh R.J et al., 1996; Zawala J et al., 2010; Wang et al., 2024; Zhu et al., 2025). Variations in pH can alter the ionization state and aggregation behavior of collectors, thereby modifying their adsorption configuration and packing density at the gas–liquid interface (Pugh at al., 1997; Lim J., 2009; Wang at al., 2024). Meanwhile, dissolved divalent cations such as Ca^{2+} and Mg^{2+}, which are ubiquitous in flotation circuits and recycled process water, may compress the electrical double layer (EDL), screen electrostatic repulsion, or react directly with anionic surfactants to form poorly soluble complexes or precipitates (Craig et al., 1993; Kume et al., 2008; Zhang et al., 2021; Fu et al., 2022). These interactions substantially affect foam generation, bubble stability, and froth persistence (Cui et al., 2022; Xu et al., 2023). Although the influence of solution chemistry on flotation systems has been widely reported, most existing studies have primarily focused on mineral surface wettability and flotation recovery (Choi et al., 2016; Bimpilas and Anastassakis., 2020; Sun et al., 2021), while the dynamic responses of collector foams themselves remain insufficiently understood.

Magnesite flotation is highly dependent on the performance of anionic collectors (Yin et al., 2010; Sun et al., 2017; Wonyen et al., 2018). Sodium oleate (NaOl), a typical fatty-acid collector, has long been used in the flotation separation of magnesite and associated gangue minerals because of its strong collecting ability toward carbonate minerals (Choi et al., 2016; Bimpilas and Anastassakis., 2020; Sun et al., 2021). More recently, cetyl phosphate (CP), a phosphate-based anionic collector, has attracted increasing attention due to its superior selectivity for calcium-bearing impurities such as dolomite and calcite (Tang et al., 2020a; Xu et al., 2020). Existing investigations on CP have mainly concentrated on adsorption mechanisms, flotation selectivity, and mineral surface interactions (Tang et al., 2020b; Tang et al., 2021). However, the dynamic foam behavior generated by CP under complex solution environments has rarely been systematically investigated. In particular, the contrasting tolerance mechanisms of phosphate- and carboxylate-type collectors toward pH variation and dissolved Ca^{2+}/Mg^{2+} ions remain unclear. This knowledge gap limits the mechanistic understanding of collector performance and restricts the optimization of flotation water chemistry under industrial conditions involving saline or recycled water systems.

The present work comparatively investigates the dynamic foam behaviors of sodium oleate and cetyl phosphate under controlled pH and divalent-ion environments. Dynamic foam analysis and surface tension measurements were employed to evaluate foamability, foam stability, and bubble evolution characteristics in the presence of varying pH and dissolved Ca^{2+}/Mg^{2+} concentrations. Particular emphasis was placed on clarifying how collector headgroup chemistry governs interfacial stability and ion tolerance. The results provide new mechanistic insights into the relationship between solution chemistry and flotation foam behavior, and they also offer theoretical guidance for collector selection and water chemistry regulation in industrial magnesite flotation systems. The results provide new mechanistic insights into the relationship between solution chemistry and collector foam behavior. These findings provide a theoretical basis for understanding the role of collector foam characteristics in magnesite flotation and optimizing reagent selection and water chemistry management.

2. Materials and methods

2.1. Materials and reagents

Sodium oleate (NaOl, analytical grade) and cetyl phosphate (CP, analytical grade, Colonial Chemical Inc., USA) were used as collectors in this study. Sodium hydroxide (NaOH) and hydrochloric acid (HCl) were employed for pH adjustment. Calcium chloride ($CaCl_2$) and magnesium chloride (MgCl2) were used as sources of Ca^{2+} and Mg^{2+}, respectively. Except for the CP collectors, all other reagents were purchased from Sinopharm Chemical Reagent Co., Ltd. (China) and used without further purification. Deionized water with a resistivity of 18.2 MΩ·cm was used throughout all experiments.

Collector stock solutions were freshly prepared prior to each experiment. The collector concentration was fixed at 40 mg/L unless otherwise specified. This concentration was selected based on the experimentally determined critical micelle concentrations (CMCs) of the two collectors. The pH of the solution was adjusted using dilute NaOH or HCl solutions and measured using a calibrated pH meter.

For ion-effect experiments, predetermined concentrations of Ca^{2+} or Mg^{2+} were introduced into the collector solution before foam measurements. The solution was stirred for 5 min to ensure sufficient equilibration prior to testing. Ca^{2+} or Mg^{2+} were selected as representative divalent ions because they are commonly present in mineral flotation circuits, particularly in recycled and saline process waters. These ions may influence anionic collector behavior through electrical double-layer regulation, specific ion–collector interactions, and the formation of insoluble metal–collector complexes. Therefore, Ca^{2+} or Mg^{2+} provide suitable models for investigating the tolerance of collector foams toward dissolved divalent ions. The concentrations of Ca^{2+} or Mg^{2+} (1, 5, 10, 20, 30, and 40 ppm) were selected to cover a trace-to-moderate ion concentration range and to systematically investigate the transition from weak electrolyte effects to severe foam destabilization caused by collector depletion and precipitation.

2.2. Surface tension measurements

Surface tension measurements were conducted using a JK99D tensiometer (Shanghai Zhongchen Digital Technology Equipment Co., Ltd., China) based on the Wilhelmy plate method. A platinum plate was cleaned with ethanol and deionized water prior to each measurement and then flamed to remove residual contaminants. Measurements were performed at 25 ± 0.5 ℃. Approximately 60 mL of solution was transferred into a glass vessel for each test. The surface tension value was recorded after the system reached equilibrium. Each measurement was repeated at least three times, and the average value was reported. The critical micelle concentration (CMC) values of NaOl and CP under different pH conditions were determined from the inflection points of the surface tension versus concentration curves (Le et al., 2019; Mabrouk et al., 2022).

2.3. Determination of dynamic foam properties

Dynamic foam properties were characterized using a Dynamic Foam Analyzer (DFA 100, KRÜSS Scientific Instruments, Germany). A schematic illustration of the measurement setup is presented in Fig. 1. The DFA measurements were performed under laboratory conditions at 25 ± 0.5 °C, and the sample temperature remained within this range throughout the measurement period. Prior to each measurement, freshly prepared collector solutions were ultrasonically degassed for 5 min using an ultrasonic bath (KQ-500E, Kunshan Ultrasonic Instruments Co., Ltd.) to remove dissolved air. Subsequently, 50 mL of the degassed solution was transferred into a transparent glass column. Foam generation was achieved by introducing compressed air through a porous sintered glass frit (G3, ~30 μm) positioned at the bottom of the column. The airflow rate was maintained at 0.30 L·min^{-1} under standard conditions (25 ℃, 1 atm). Aeration was conducted for 30 s, after which the airflow was terminated. Foam decay behavior was subsequently monitored for 30 min.

Foam parameters were extracted from the foam height–time profiles. Foamability was evaluated using the maximum foam height (Hmax) measured immediately after aeration. Foam stability was characterized by the foam half-life (t1/2), defined as the time required for the foam height to decrease to 50% of Hmax (Arellano et al., 2017). Bubble evolution was monitored using the integrated image analysis module of the DFA100 instrument. Bubble size was characterized using the mean equivalent diameter calculated from the projected two-dimensional bubble area. The equivalent diameter was selected because it provides a representative description of irregular foam bubbles generated during dynamic foam evolution. Since the image analysis was based on projected bubble areas, area-weighted statistics were applied rather than volume-weighted calculations. For each experimental condition, representative images were automatically analyzed, and more than 200 individual bubbles were identified to obtain statistically reliable bubble size distributions. The temporal variation of the mean equivalent bubble diameter was subsequently used to evaluate bubble coalescence and foam structural evolution. Meanwhile, the pH-dependent foam experiments were conducted within the pH range of 4–11. This range was selected according to the acid–base dissociation characteristics of the investigated collectors and the practical alkaline conditions commonly encountered in magnesite flotation systems. The selected pH range covers the major protonation and ionization states of both collectors. Specifically, acidic conditions (pH 4–6), near-neutral conditions (pH 7–9), and alkaline conditions (pH 10–11) were employed to evaluate the effects of protonation, optimal ionic-species formation, and excessive ionization-induced electrostatic repulsion on collector foam stability.

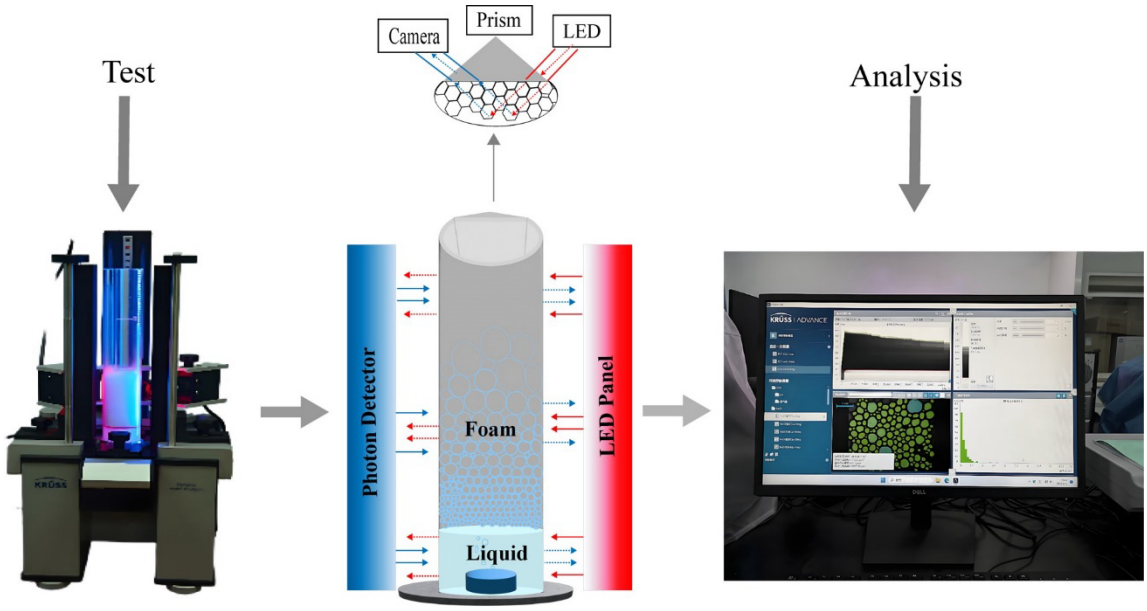

Fig. 1. Schematic diagram of the equipment principle.

3. Results and discussion

3.1. Influence of solution environment on surface tension

Surface tension is a crucial interfacial property that governs the dynamic behavior of flotation froth (Kanokkarn et al., 2017; Xing et al., 2017; Wen et al., 2024). Under natural pH conditions—measured as 6.8 for CP and 8.2 for NaOl—the surface tension of both collectors decreased with increasing concentration, exhibiting a classic two-stage trend indicative of micellization (Fig. 2a). The surface tension plateaued at ~41.40 mN·m-1 for CP and ~28.70 mN·m-1 for NaOl, corresponding to critical micelle concentrations (CMCs) of 0.04 wt.% and 0.02 wt.%, respectively. The consistently lower surface tension of NaOl solutions suggests its superior intrinsic foamability compared to CP (Atrafi and Pawlik., 2016). Solution pH profoundly influences surfactant molecular configuration and dissociation. Increasing the pH from 4 to 11 reduced the surface tension for both collectors (Fig. 2b), with NaOl demonstrating greater sensitivity to pH variation. This reduction is directly linked to increased dissociation of the collector headgroups. For carboxylic acids like NaOl, when pH exceeds the pKa (~4.96), the molecules predominantly exist as negatively charged oleate ions (Ol^-), which adsorb more efficiently at the air-water interface (Jisung and Lim., 2009; Xie et al., 2020). Notably, the surface tension of CP increased under both highly acidic (pH < 4) and strongly alkaline (pH > 10) conditions. This can be attributed to the speciation of CP: protonation to the neutral form ($C_{16}H_{33}OPO_3H_2$) at low pH reduces solubility, while excessive dissociation to the dianion ($C_{16}H_{33}OPO_3^{2-}$) at high pH increases electrostatic repulsion, both impairing efficient interfacial packing.

The introduction of divalent cations (Ca^{2+}, Mg^{2+}) increased the surface tension of both collector solutions in a concentration-dependent manner (Figs. 2c and 2d), indicating a common detrimental response. This increase is attributed to two concurrent mechanisms: (i) charge neutralization between cations and anionic headgroups, which reduces the effective concentration of active surfactant monomers, and (ii) complexation leading to the formation of insoluble metal-soap precipitates (Lan et al., 2025). In the foam system, these effects manifest as accelerated drainage of the lamellae and enhanced bubble coalescence, phenomena directly linked to the observed increase in surface tension. Consequently, elevated concentrations of divalent cations raise the surface tension, creating conditions unfavorable for the formation and stabilization of froth.

3.2. Influence of solution environment on dynamic foam properties

Dynamic foam properties are critical determinants of flotation efficiency. Parameters such as maximum foam height and foam half-life directly quantify foamability and foam stability, respectively (Chen and

Tao., 2004; Li et al., 2016). Using dynamic foam analysis, this study reveals the stability mechanisms of CP and NaOl by monitoring the temporal evolution of foam height, half-life ($t_1/_2$), and bubble size distribution under varying solution conditions.

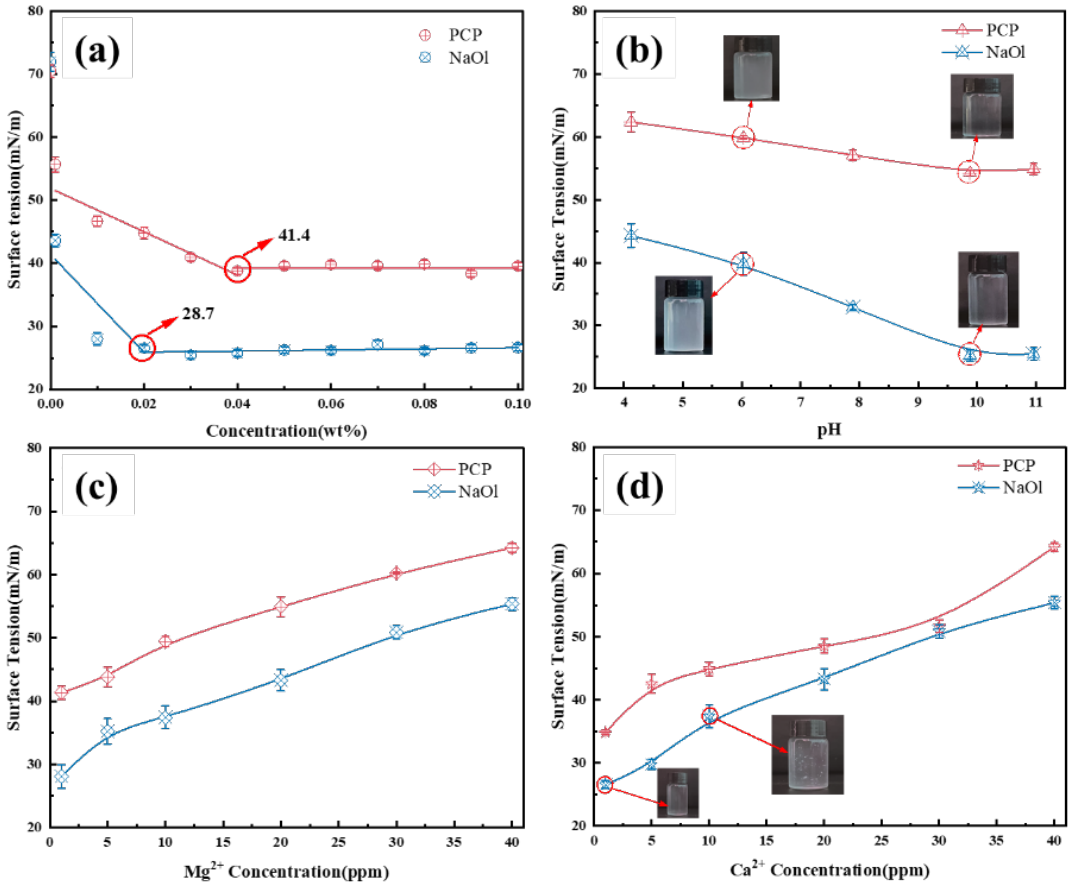

Fig. 2. Effect of solution environment on the surface tension of collectors

3.2.1. Effect of pH

The dynamic foam behaviors of CP and NaOl exhibited markedly different responses to pH variation, reflecting the distinct dissociation characteristics and intermolecular interactions of phosphate- and carboxylate-type collectors. The pH-dependent speciation distributions of both collectors were calculated according to their acid dissociation constants and are presented in Fig. 3. CP undergoes two-step dissociation in aqueous solution, with pK1 ≈ 2.02 and pK2 ≈ 7.49, whereas NaOl exhibits single-step dissociation with a pKa of approximately 4.96 (Kinoshita et al., 2018; Tang et al., 2026). Consequently, the dominant CP species gradually changes from the neutral molecular form ($C_{16}H_{33}OPO_3H_2$) under strongly acidic conditions to the monoanionic species ($C_{16}H_{33}OPO_3H^-$) near neutral pH, and finally to the fully dissociated dianion ($C_{16}H_{33}OPO_3^{2-}$) under alkaline conditions. In contrast, NaOl mainly exists as oleate ions (Ol^-) above pH 4.96, while protonation below this pH promotes the formation of neutral oleic acid species.

These speciation differences strongly influenced foam generation and stability behavior (Figs. 4–7). Under alkaline conditions, NaOl exhibited significantly superior foamability compared with CP. At pH 9.9 and 10.9, the maximum foam heights reached approximately 160 and 157 mm, respectively (Fig. 4a), accompanied by relatively stable foam growth rates. The enhanced foam stability under alkaline conditions can be attributed to the strong interfacial adsorption of dissociated oleate ions. The negatively charged carboxylate headgroups promote the formation of a cohesive and electrostatically stabilized interfacial film, thereby suppressing liquid drainage and bubble coalescence (Jisung and Lim., 2009; Xie et al., 2020). In addition, the fully dissociated oleate species exhibit improved molecular dispersion in solution, facilitating continuous adsorption at newly generated gas–liquid interfaces during foam formation.

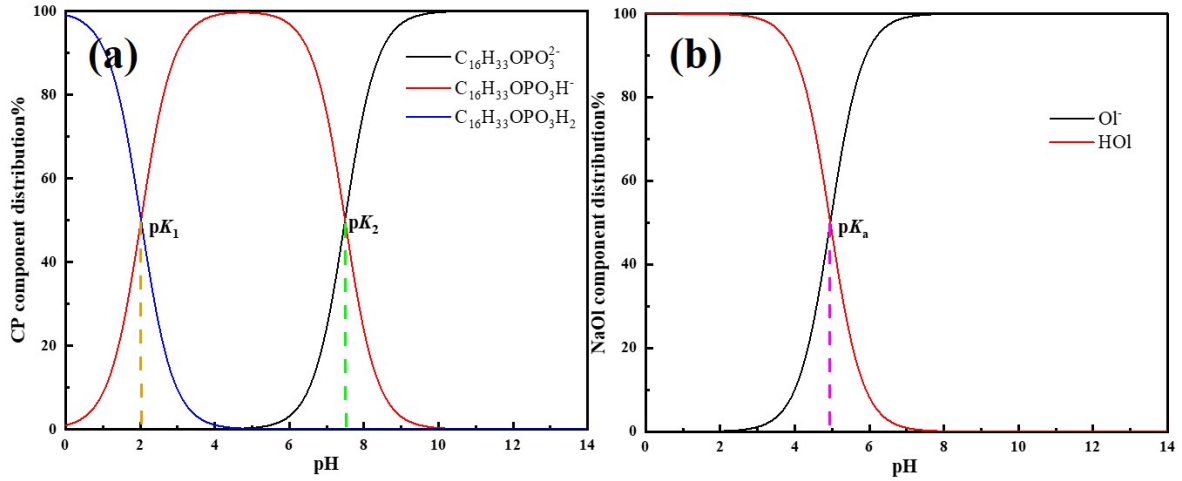

Fig. 3. Composition distribution of CP and NaOl at different pH values (a. CP; b. NaOl)

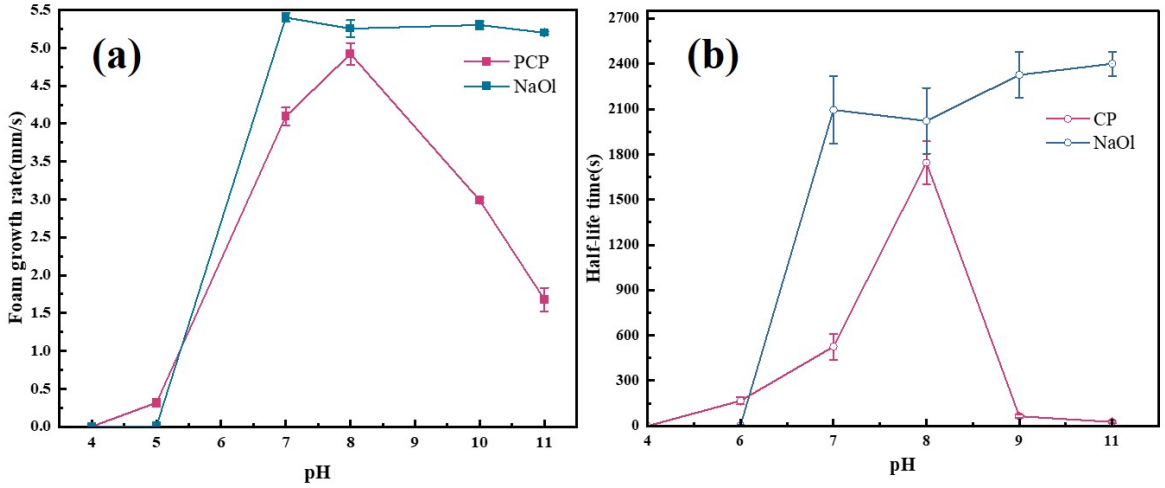

Fig. 4. Effects of pH values on the foaming and stability of two types of collector solutions. (a. foam growth rate; b. foam half-life)

In contrast, CP exhibited optimal foaming performance near pH 8, where the maximum foam height reached approximately 124 mm. In this pH range, the monoanionic phosphate species dominated the solution chemistry and provided a favorable balance between electrostatic repulsion and intermolecular cohesion. This balance may favor a relatively compact interfacial organization and stabilized medium-sized bubbles over extended periods. However, CP foam stability deteriorated rapidly under strongly alkaline conditions (pH > 10). The transition from monoanionic to dianionic phosphate species substantially increased electrostatic repulsion between adjacent headgroups, weakening intermolecular cohesion within the adsorption layer and suggests reduced film elasticity. As a result, accelerated film drainage and bubble coalescence occurred, leading to rapid foam collapse. The foam volume decreased by nearly 30% within the first 10 min at pH 11 (Fig. 5a), indicating severe destabilization of the foam structure.

Acidic conditions produced distinctly different destabilization mechanisms for the two collectors. For CP, strong protonation under acidic conditions converted the phosphate species into the neutral molecular form ($C_{16}H_{33}OPO_3H_2$), which significantly weakened its amphiphilic character and interfacial activity. Consequently, the average bubble size increased markedly to approximately 400–450 μm, and the resulting foam rapidly collapsed within 10 min (Fig. 6a). The enlarged and unstable bubble structure suggests that neutral CP molecules were unable to form sufficiently cohesive adsorption films at the gas–liquid interface, thereby accelerating bubble coalescence and lamella rupture. Nevertheless, CP retained partial foamability down to pH ~4 because the first dissociation equilibrium still allowed a fraction of monoanionic phosphate species to remain in solution.

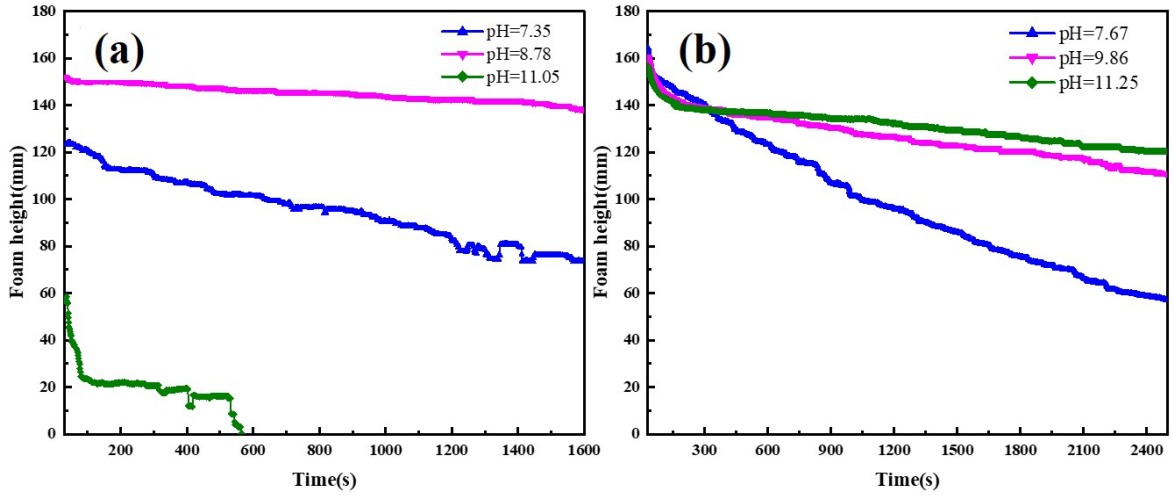

Fig. 5 Changes in the decay curves of foams at different pH values. (a. CP solution; b. NaOl solution)

For NaOl, foamability sharply deteriorated below pH 7.7 and completely disappeared under more acidic conditions. This behavior cannot be explained solely by simple protonation. Instead, the reduction in foam stability is more plausibly associated with the formation of hydrophobic acid–soap aggregates and oleic acid precipitation (Shu et al., 2014). Protonation decreases collector solubility and reduces the concentration of surface-active oleate monomers available for interfacial adsorption. Simultaneously, the loss of electrostatic repulsion between bubble surfaces accelerates film thinning and coalescence, ultimately causing immediate collapse of the foam structure. Compared with CP, NaOl therefore exhibited substantially lower tolerance toward acidic environments.

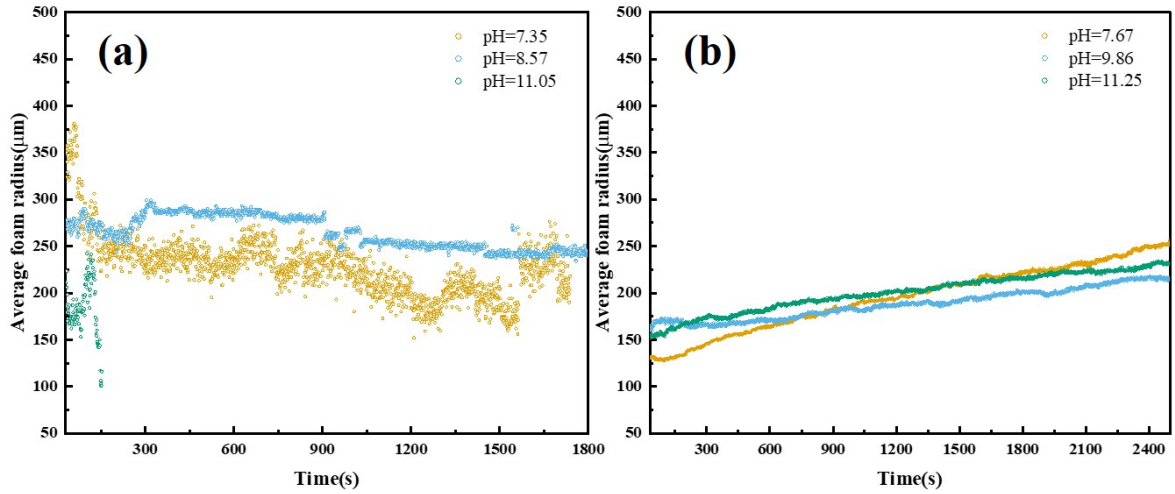

Fig. 6 Effect of pH on foam size (a. CP; b. NaOl)

Bubble evolution analysis further supported the distinct stabilization mechanisms of the two collectors. Near neutral pH, CP maintained relatively stable bubble sizes of approximately 300 μm with limited fluctuation over time, indicating a dynamic balance between bubble coalescence and rupture. In contrast, NaOl generated smaller and more uniformly distributed bubbles under alkaline conditions, with average bubble sizes ranging from 125 to 175 μm (Fig. 6b). The smaller bubble size distribution reflects the stronger electrostatic stabilization provided by dissociated oleate ions, which effectively inhibited uncontrolled coalescence during foam aging.

The temporal evolution profiles shown in Fig. 7 visually corroborate these mechanistic differences. For CP, stable foam structures were sustained only within a relatively narrow near-neutral pH range, whereas rapid structural degradation occurred under both strongly acidic and strongly alkaline conditions. By comparison, NaOl maintained a more persistent and coherent foam network under alkaline conditions but underwent abrupt structural collapse once protonation and aggregation became

dominant at lower pH values. These observations collectively demonstrate that the pH tolerance of flotation foams is fundamentally governed by collector headgroup chemistry, which modulates surfactant speciation, intermolecular interaction, and interfacial film stability under different solution environments.

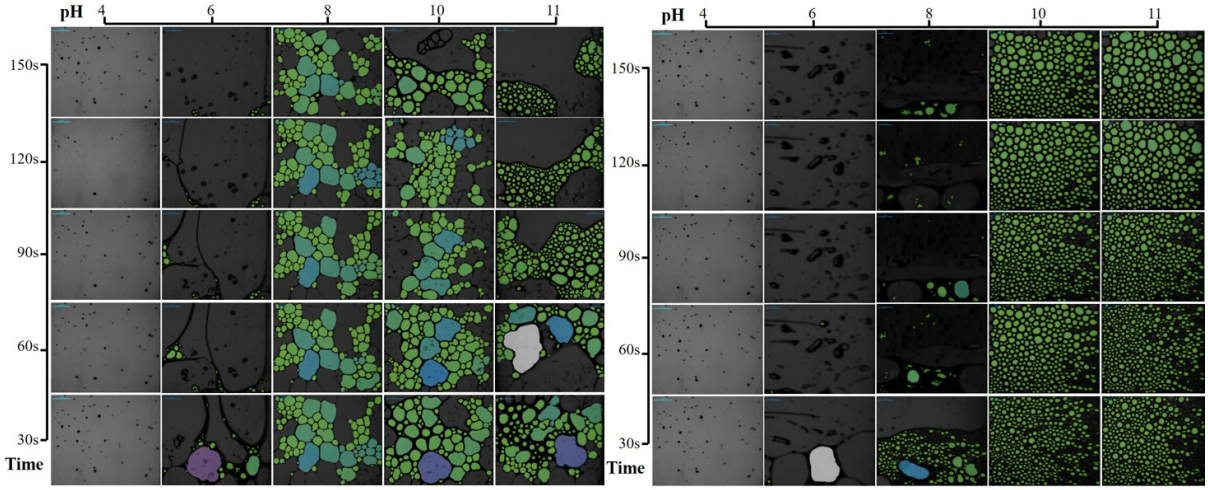

Fig. 7 Dynamic behavior changes of foam with pH values (a. CP; b. NaOl)

3.2.2. Effect of Mg^{2+} concentration

The dynamic foam behaviors of CP and NaOl exhibited distinctly different responses to Mg^{2+} concentration, reflecting the different interaction mechanisms between Mg^{2+} and the phosphate- and carboxylate-type collector headgroups (Figs. 8–11). Mg^{2+} produced relatively moderate effects on foam stability over a broader concentration range, indicating weaker coordination interactions and slower interfacial destabilization kinetics.

For CP, low Mg^{2+} concentrations produced a slight enhancement in foam stability. As shown in Fig. 8a, the maximum foam height increased moderately at Mg^{2+} concentrations below approximately 20 ppm, while the foam decay rate simultaneously decreased (Fig. 9a). This behavior suggests that moderate Mg^{2+} addition partially improved the stability of the interfacial adsorption layer. At relatively low concentrations, Mg^{2+} ions can compress the electrical double layer (EDL) surrounding adjacent phosphate headgroups, thereby reducing excessive electrostatic repulsion within the adsorption film. The weakened repulsive interaction may favor closer intermolecular organization and thereby contribute to greater resistance to bubble coalescence and liquid drainage (Schelero et al., 2010; Xie et al., 2017; Petkova et al., 2020; Lan et al., 2025). Bubble evolution analysis further supports this stabilization mechanism. At low Mg^{2+} concentrations, CP foam maintained relatively uniform bubble populations with average bubble diameters remaining within a comparatively narrow range during foam aging (Fig. 10a). The suppression of rapid bubble coalescence indicates that moderate EDL compression contributed to dynamic stabilization of the foam structure. Similar ion-induced stabilization phenomena have also been reported in other anionic surfactant foam systems, where moderate electrolyte concentrations improve intermolecular packing at the interface (Xie et al., 2017; Kedir et al., 2022). However, as the Mg^{2+} concentration increased further, the stabilization effect gradually disappeared and was replaced by progressive foam destabilization. At Mg^{2+} concentrations exceeding approximately 50 ppm, both foam height and foam half-life decreased noticeably (Figs. 8a and 8b), accompanied by accelerated foam collapse after aeration ceased (Fig. 9a). This transition appears to reflect a shift in the dominant destabilization mechanism from moderate EDL regulation a possible reduction in the availability of surface-active collector species and disruption of the interfacial adsorption structure.

The deterioration of CP foam stability at elevated Mg^{2+} concentrations is likely associated with ion-induced interactions between Mg^{2+} and phosphate headgroups, which may promote the formation of

magnesium-containing phosphate species and reduce the availability of surface-active CP molecules. Although Mg^{2+} possesses the strong hydration of Mg^{2+} may limit its direct interaction with phosphate-containing headgroups, increasing ion concentrations may facilitate partial dehydration of Mg^{2+} and enhance its interaction probability with oxygen-containing phosphate groups (Xie et al., 2017). The resulting reduction in free collector concentration decreases the availability of surface-active species for interfacial adsorption. Simultaneously, excessive ion accumulation near the interface may disturb the uniform arrangement of phosphate headgroups and weaken film elasticity. Consequently, liquid drainage and bubble coalescence become increasingly pronounced during foam aging (Yamanaka., 1975; Wang and Yoon., 2009).

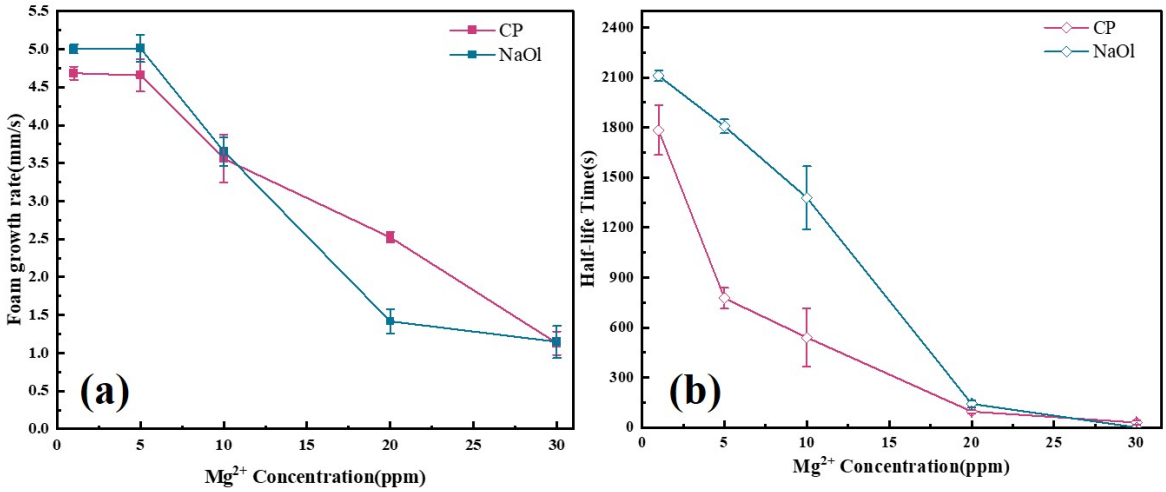

Fig. 8 The effect of Mg^{2+} concentration on the foaming and stability of the collector (a. foam growth rate; b. foam half-life)

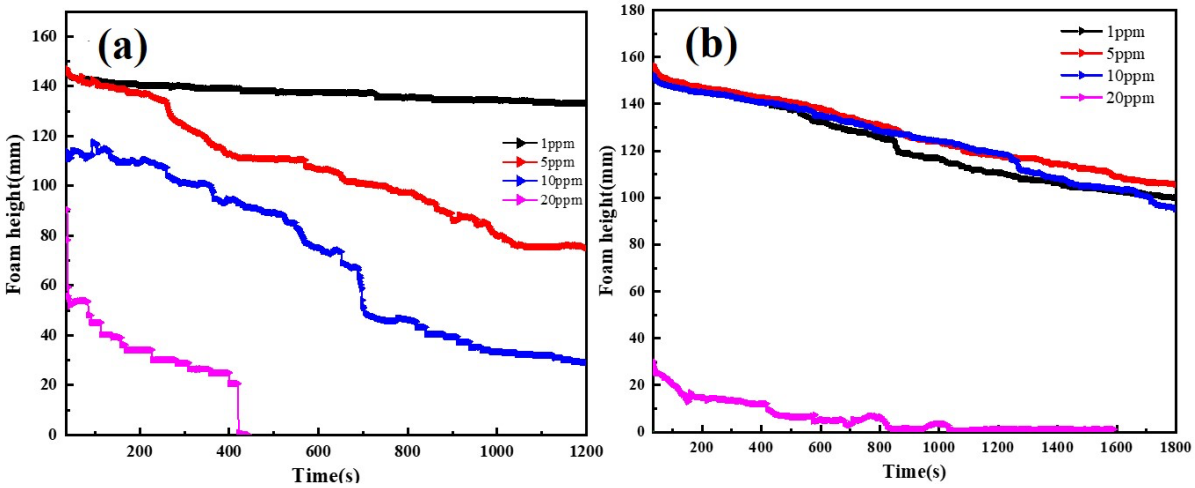

Fig. 9 The change in foam height of collector solutions at different Mg^{2+} concentrations over time (a. CP; b. NaOl)

The bubble evolution behavior shown in Fig. 10a reflects this progressive destabilization process. Under elevated Mg^{2+} concentrations, bubble size distributions became increasingly non-uniform, and larger bubbles gradually dominated the foam structure. This phenomenon appears to reflect a gradual weakening of the stabilization capacity of the interfacial adsorption layer as surfactant depletion and film disruption intensify. Nevertheless, compared with the Ca^{2+} system discussed later, the destabilization induced by Mg^{2+} remained relatively gradual and did not immediately destroy the entire foam structure.

NaOl exhibited a different response pattern toward Mg^{2+} concentration. Compared with CP, the NaOl foam system maintained relatively stable foamability over a wider Mg^{2+} concentration range (Figs. 8c and 8d). The maximum foam height and foam half-life showed only moderate reductions at low-to-

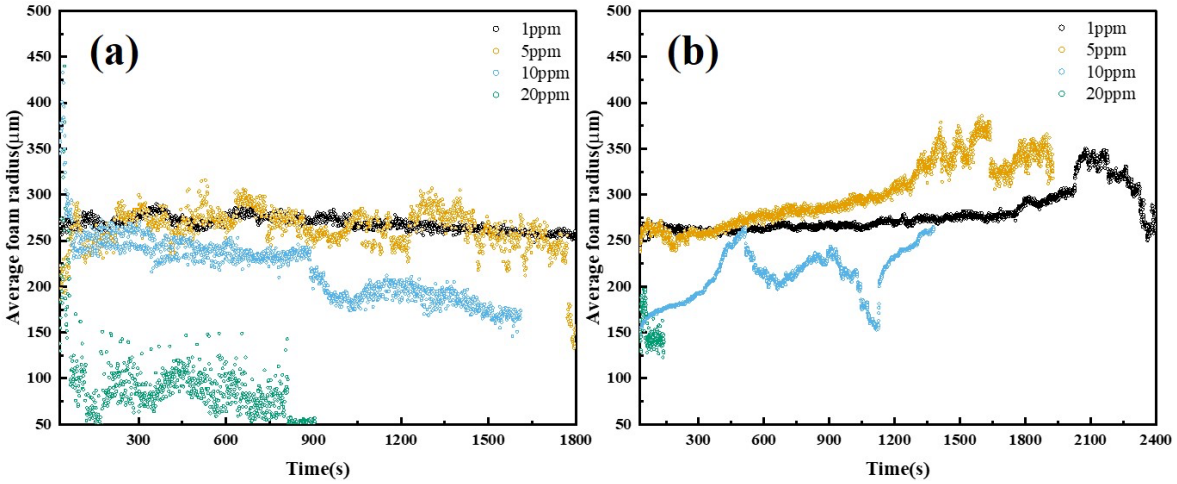

Fig. 10 Effect of different Mg^{2+} concentrations on foam size (a. CP; b. NaOl)

medium Mg^{2+} concentrations, indicating comparatively stronger tolerance of the oleate-based foam system toward Mg^{2+} ions. This behavior may be largely related to the different coordination characteristics of carboxylate headgroups. The interaction between Mg^{2+} and oleate species is relatively weaker than that between Mg^{2+} and phosphate groups because the strongly hydrated Mg^{2+} ions are less likely to form stable inner-sphere complexes with carboxylate oxygen atoms. Consequently, moderate Mg^{2+} concentrations mainly influence the NaOl foam system through EDL compression rather than rapid surfactant precipitation. Under such conditions, the electrostatic repulsion between adjacent oleate headgroups is partially reduced, which may temporarily promote intermolecular packing within the adsorption film (Xie et al., 2017; Binks and Shi., 2020).

At higher Mg^{2+} concentrations, however, gradual destabilization of the NaOl foam system still became apparent. The foam decay profiles shown in Fig. 9b demonstrate increasing collapse rates with increasing Mg^{2+} concentration, while the average bubble size simultaneously increased during foam aging (Fig. 10b). This behavior suggests that excessive Mg^{2+} accumulation eventually weakened the interfacial stabilization provided by oleate adsorption. The formation of magnesium oleate species and the reduction in free oleate concentration likely contributed to the deterioration of foam stability under these conditions.

The spatiotemporal foam evolution profiles shown in Fig. 11 further illustrate the different Mg^{2+}-tolerance characteristics of the two collectors. CP exhibited an initial stabilization region at low Mg^{2+} concentrations followed by gradual destabilization at higher concentrations, whereas NaOl maintained relatively persistent foam structures over a broader ion concentration range. These observations collectively indicate that Mg^{2+} influences anionic collector foams through a concentration-dependent transition from moderate electrostatic regulation to progressive surfactant depletion and interfacial disruption. The relatively strong hydration shell of Mg^{2+} moderates direct coordination interactions and therefore delays catastrophic foam collapse compared with Ca^{2+} systems (Wang and Yoon., 2009).

3.2.3. Effect of Ca^{2+} concentration

The influence of Ca^{2+} on the dynamic foam properties of CP and NaOl differed substantially from that of Mg^{2+}, exhibiting significantly stronger destabilizing effects on both collector systems, particularly for CP (Figs. 12–15). Compared with Mg^{2+}, Ca^{2+} induced more rapid deterioration of foamability, foam stability, and bubble structural integrity, indicating fundamentally different interaction mechanisms between the divalent cations and collector headgroups.

CP exhibited pronounced sensitivity toward dissolved Ca^{2+}. Even at a Ca^{2+} concentration of only 1 ppm, the maximum foam height decreased sharply to below 70 mm (Fig. 12a), while the foam half-life was reduced to less than 4.5 min (Fig. 12b). Simultaneously, the foam decay profiles shown in Fig. 13a revealed rapid collapse immediately after aeration ceased, indicating that the foam structure was unable to maintain dynamic stability even over short timescales. This behavior contrasts sharply with the Mg^{2+}

system, where low ion concentrations still preserved partial foam stabilization through electrical double layer (EDL) compression effects (Craig et al., 1993. Li et al., 2016).

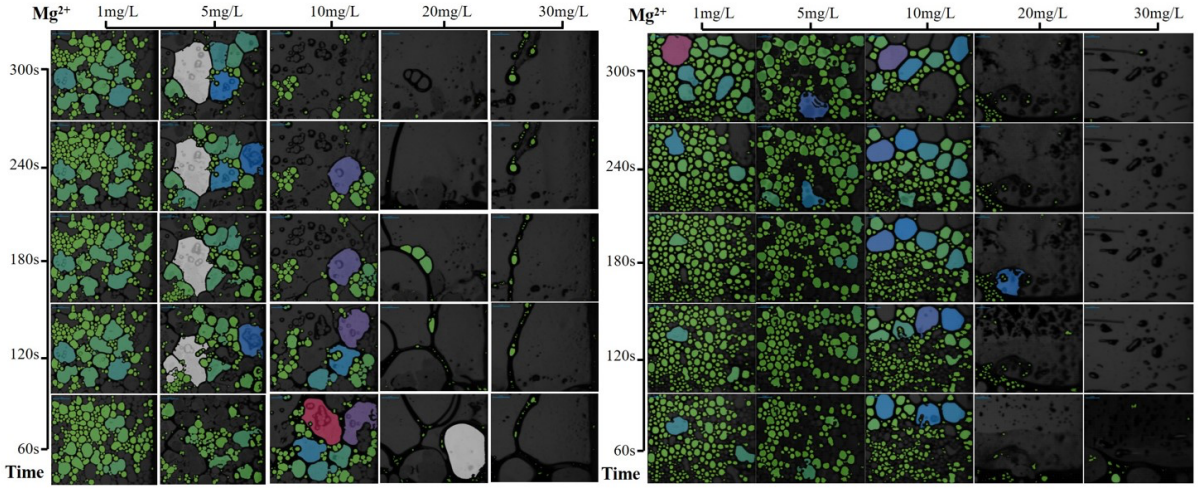

Fig. 11 Dynamic behavior changes of foam with Mg^{2+} concentration (a. CP; b. NaOl)

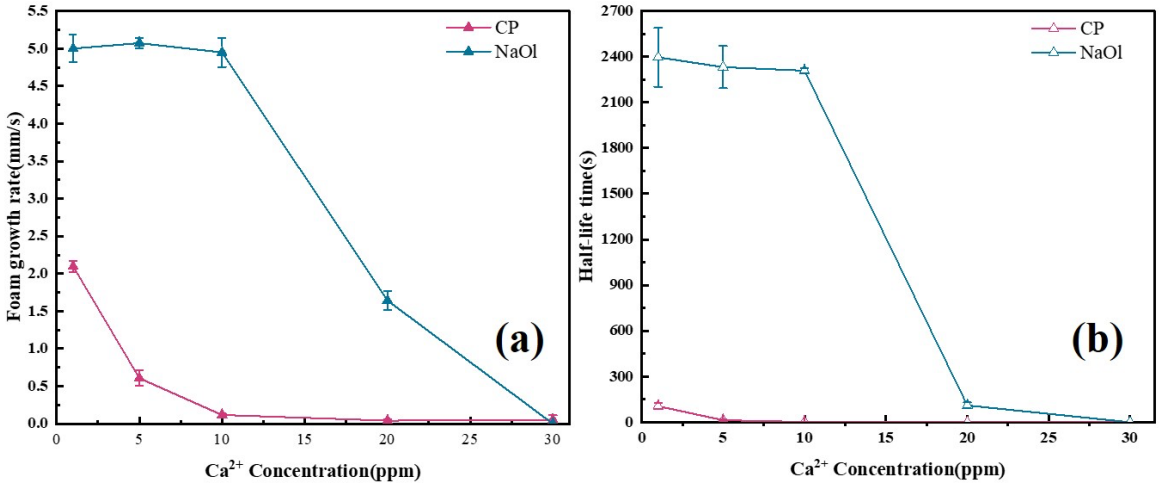

Fig. 12 The effect of Ca^{2+} concentration on the foaming and stability of collectors (a. foam growth rate; b. foam half-life)

The severe destabilization of CP foam is likely attributed to the stronger interaction tendency between Ca^{2+} and phosphate headgroups compared with Mg^{2+}, which may accelerate the depletion of interfacially active CP species. Unlike Mg^{2+}, Ca^{2+} possesses a weaker hydration shell and lower hydration energy, which facilitate partial dehydration and promote inner-sphere complexation with phosphate oxygen atoms (Lan et al., 2025). As a result, highly insoluble calcium phosphate–collector complexes form rapidly in solution and at the gas–liquid interface, causing substantial depletion of surface-active CP molecules. The rapid loss of interfacially adsorbed surfactants weakens film elasticity, accelerates lamella drainage, and promotes bubble coalescence and rupture (Fu et al., 2022; Peng et al., 2024). Furthermore, Ca^{2+} may also act as a bridging species between adjacent phosphate headgroups, inducing excessive intermolecular aggregation and disrupting the uniformity of the adsorption layer. These combined effects ultimately lead to catastrophic collapse of the foam structure even at trace Ca^{2+} concentrations.

Bubble evolution analysis further confirmed the severe interfacial destabilization induced by Ca^{2+}. As shown in Fig. 14a, CP foam exhibited highly disordered bubble size distributions accompanied by rapid disappearance of the foam phase. Because the foam volume became extremely limited after aeration, the remaining bubble size variations primarily reflected unstable coalescence events rather

than a dynamically stabilized foam structure. This behavior differs fundamentally from the relatively stable bubble populations observed under Mg^{2+} environments, further demonstrating the exceptional sensitivity of phosphate-based collectors toward calcium ions (Chen and Tao., 2004; Li et al., 2016).

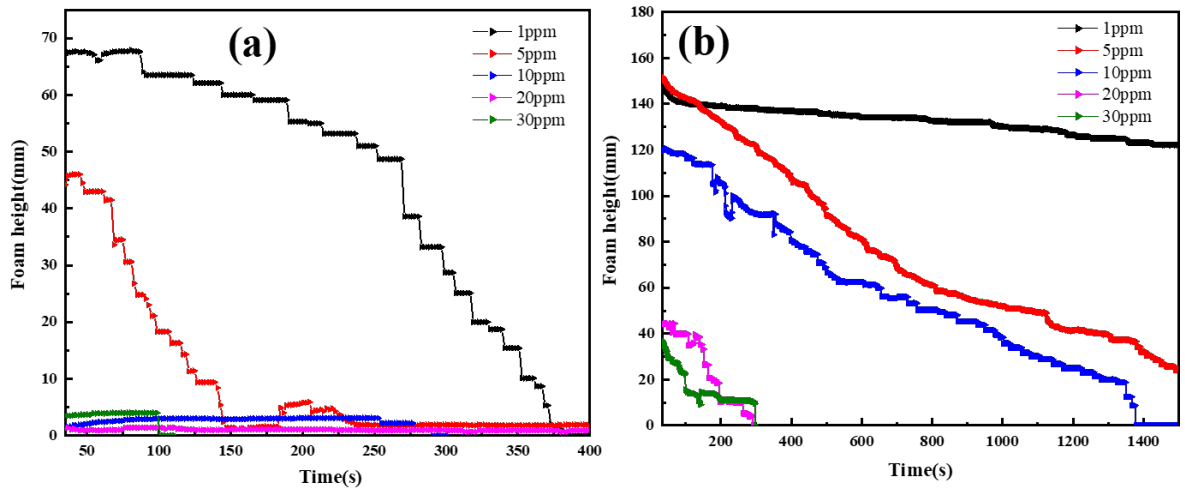

Fig. 13 The change in foam height of collector solutions at different Ca^{2+} concentrations over time (a. CP; b. NaOl)

In contrast to CP, NaOl exhibited substantially greater tolerance toward Ca^{2+} at low ion concentrations. At 1–10 ppm Ca^{2+}, the foam system still maintained relatively high foam heights and moderate foam half-lives (Figs. 12a and 12b), suggesting that severe interfacial disruption had not yet occurred. Under these conditions, moderate EDL compression likely reduced electrostatic repulsion between oleate headgroups and slightly enhanced intermolecular packing within the adsorption layer (Craig et al., 1993; Shu et al., 2014). Consequently, relatively stable foam structures and bubble populations were maintained during the initial stages of foam aging.

However, once the Ca^{2+} concentration exceeded approximately 20 ppm, the NaOl foam system underwent rapid destabilization. The foam height and foam half-life decreased sharply, accompanied by substantial reductions in bubble number density (Fig. 13b). This deterioration is primarily associated with extensive precipitation of calcium oleate species. Compared with phosphate groups, the carboxylate headgroups of NaOl exhibit weaker coordination affinity toward Ca^{2+}, allowing the collector system to tolerate moderate calcium concentrations before precipitation becomes dominant (Shu et al., 2014). Nevertheless, once the precipitation threshold is exceeded, rapid consumption of oleate ions significantly reduces the concentration of surface-active monomers available for interfacial adsorption, thereby destabilizing the foam structure.

The bubble evolution behavior of NaOl further illustrates this concentration-dependent transition. At low Ca^{2+} concentrations, the average bubble size remained relatively uniform within the range of 200–300 μm (Fig. 14b), indicating that bubble coalescence was still effectively suppressed. At elevated Ca^{2+} concentrations, although the overall foam stability deteriorated markedly, the bubble size increase remained less dramatic than that observed for CP. This suggests that the destabilization mechanism of NaOl is dominated primarily by surfactant depletion through precipitation rather than catastrophic interfacial film collapse. Consequently, the NaOl foam system retained partial structural coherence even under relatively harsh calcium conditions.

The spatiotemporal evolution profiles shown in Fig. 15 visually corroborate these mechanistic differences. For CP, the foam matrix underwent near-instantaneous structural failure even at trace Ca^{2+} levels, reflecting the rapid Ca^{2+}-induced loss of foam stability, possibly associated with Ca^{2+}–phosphate interactions and reduced availability of surface-active CP species. In contrast, NaOl maintained a relatively coherent foam structure at low Ca^{2+} concentrations, while severe structural degradation became apparent only after possible formation or precipitation of calcium–oleate species occurred at higher ion concentrations. These observations collectively demonstrate that Ca^{2+} is a substantially more aggressive destabilizing ion than Mg^{2+} for anionic collector foams, and that collector tolerance toward

calcium ions is fundamentally governed by headgroup coordination chemistry and precipitation propensity (Shu et al., 2014; Lan et al., 2025).

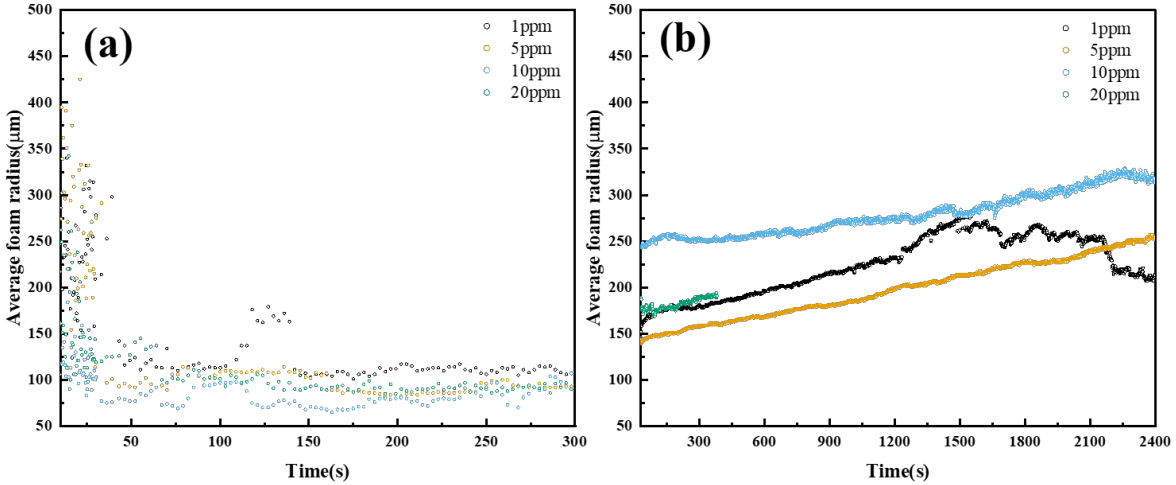

Fig. 14 Effect of different Ca^{2+} concentrations on foam size (a. CP; b. NaOl)

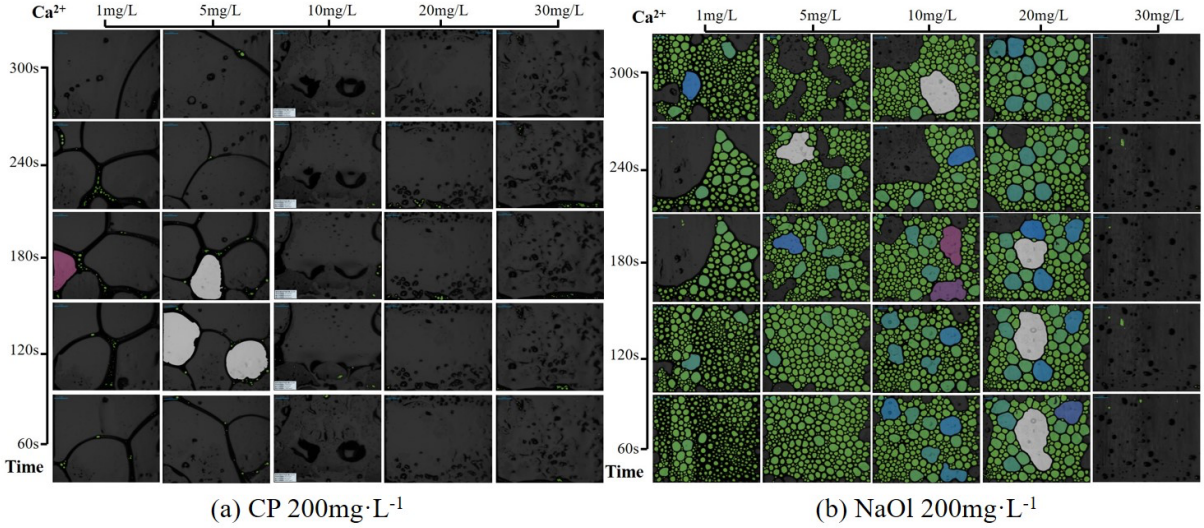

Fig. 15 Dynamic behavior changes of foam with Ca^{2+} concentration (a. CP; b. NaOl)

3.3. Mechanistic overview of solution-chemistry-dependent foam stability

The experimental results collectively demonstrate that the dynamic foam stability of anionic collectors is fundamentally governed by the coupling relationship between collector headgroup chemistry and solution environment. As illustrated schematically in Fig. 16, pH variation and dissolved divalent cations regulate flotation foam behavior through three interrelated mechanisms: collector speciation, electrostatic interaction, and ion-induced complexation/precipitation. The relative dominance of these mechanisms determines the interfacial stability, bubble evolution behavior, and macroscopic foam persistence of the collector systems.

Under ion-free conditions, pH primarily controls the dissociation state and interfacial adsorption behavior of the collectors. For NaOl, alkaline environments may promote the formation of dissociated oleate ions, which are expected to adsorb at the gas–liquid interface and give rise to electrostatically stabilized interfacial films. The associated intermolecular cohesion and surface charge repulsion would likely suppress bubble coalescence and maintain relatively stable foam structures over extended periods. However, under acidic conditions, protonation of oleate ions promotes the formation of neutral oleic acid species and hydrophobic acid–soap aggregates, leading to reduced collector solubility and severe loss of interfacial activity. Consequently, foam stability deteriorates rapidly once protonation

becomes dominant. In contrast, CP exhibits a narrower pH stability window because of its two-step dissociation behavior. Near neutral pH, the monoanionic phosphate species appear to provide an optimal balance between intermolecular cohesion and electrostatic repulsion, likely enabling relatively compact adsorption packing and stable foam formation. Under strongly alkaline conditions, the transformation to fully dissociated dianionic phosphate species would likely strengthen headgroup repulsion, weakens adsorption layer cohesion, and accelerates film drainage and bubble coalescence. Under strongly acidic conditions, protonation converts CP into neutral molecular species with insufficient amphiphilic character to maintain stable interfacial adsorption. As a result, CP foam stability becomes highly sensitive to pH-induced changes in phosphate speciation.

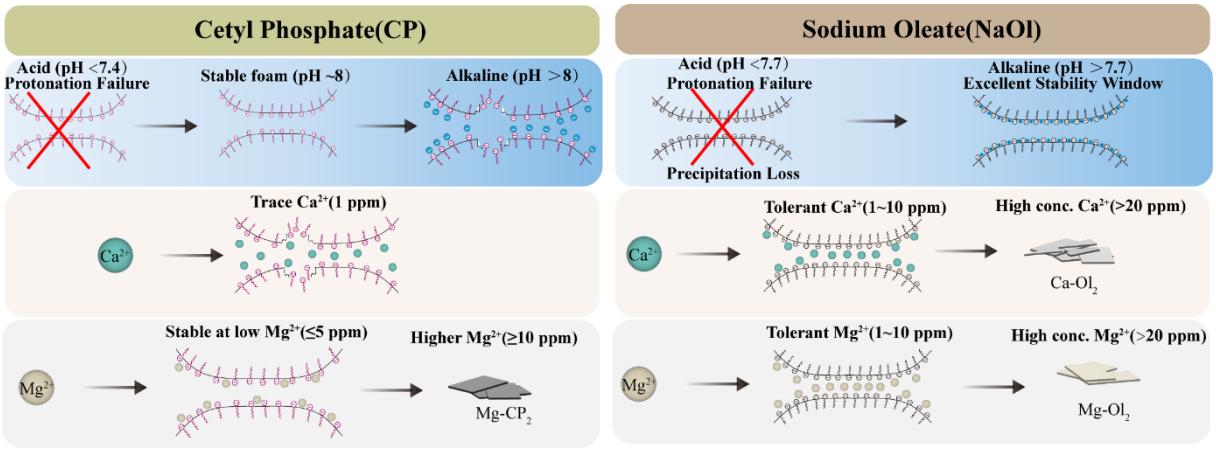

Fig. 16 Schematic diagram of the collector tolerance mechanism under different solution environments

When divalent cations are introduced into the system, ion-specific interactions become increasingly dominant. At relatively low Mg^{2+} concentrations, moderate compression of the electrical double layer (EDL) would likely partially reduces electrostatic repulsion between adjacent anionic headgroups and may temporarily improve intermolecular packing, particularly for CP. However, as the Mg^{2+} concentration increases, ion-induced surfactant depletion and interfacial disruption gradually dominate the foam destabilization process. The strong hydration shell of Mg^{2+} limits direct coordination with anionic headgroups to some extent, thereby moderating precipitation kinetics and delaying catastrophic foam collapse. Compared with Mg^{2+}, Ca^{2+} exhibits substantially stronger destabilizing capability because of its lower hydration energy and greater tendency toward partial dehydration and inner-sphere coordination. The weaker hydration shell facilitates direct interaction between Ca^{2+} and anionic collector headgroups, promoting the rapid formation of poorly soluble calcium–collector complexes. This effect is particularly severe for phosphate-based collectors such as CP, whose multiple coordinating oxygen atoms strongly favor calcium binding. Rapid surfactant depletion, excessive intermolecular aggregation, and loss of interfacial elasticity collectively induce catastrophic foam collapse even at trace Ca^{2+} concentrations. By comparison, the weaker coordination affinity between Ca^{2+} and carboxylate groups allows NaOl to retain partial tolerance toward moderate calcium concentrations before extensive calcium oleate precipitation occurs. These observations collectively indicate that flotation foam stability is not governed solely by conventional surface tension effects, but rather by the dynamic coupling among surfactant speciation, interfacial adsorption structure, electrostatic interaction, and ion-specific coordination chemistry. The distinct tolerance behaviors of phosphate- and carboxylate-type collectors therefore originate fundamentally from differences in headgroup coordination characteristics and interfacial assembly behavior under varying solution environments.

The high Ca^{2+} sensitivity of CP suggests that Ca^{2+} removal (e.g., by precipitation or ion ex-change) is necessary when using CP in hard or recycled water. For NaOl, which tolerates up to ~10 ppm Ca^{2+}, alkaline pH adjustment may be more cost-effective. These findings highlight the importance of matching collector selection to water chemistry. From an industrial perspective, the present findings highlight the critical importance of water chemistry regulation in flotation systems employing anionic collectors. In saline or recycled water environments containing elevated concentrations of dissolved Ca^{2+} and Mg^{2+}, collector selection and pH control become essential for maintaining froth stability and

flotation efficiency. The mechanistic framework established in this study provides theoretical guidance for optimizing flotation reagent schemes and improving process adaptability under complex water-quality conditions. From an industrial water management perspective, the present findings suggest that controlling dissolved divalent cations should be considered an essential strategy for maintaining froth stability in recycled-water flotation circuits. Since Ca^{2+} exhibited a significantly stronger destabilizing effect than Mg^{2+}, particularly for phosphate-based collectors such as CP, priority should be given to monitoring and regulating Ca^{2+} accumulation during process water recycling.

It should be noted that the present study mainly evaluates the intrinsic foam behavior of collector solutions under different aqueous conditions. Although foam stability is an important factor influencing flotation performance, stable foam formation alone does not necessarily indicate efficient mineral flotation. Therefore, the present results provide fundamental insights into collector–solution interactions and foam stability mechanisms, but further flotation experiments using mineral particles are required to establish the quantitative relationship between collector foam characteristics and flotation efficiency.

4. Conclusions

This study systematically investigated the effects of pH and dissolved Ca^{2+}/Mg^{2+} ions on the dynamic foam behaviors of sodium oleate (NaOl) and cetyl phosphate (CP), aiming to clarify the role of collector structure and solution chemistry in froth stability during magnesite flotation.

(1) The foam stability of NaOl and CP exhibited distinct pH-dependent behaviors. NaOl showed superior foam performance under alkaline conditions due to enhanced oleate ion adsorption, whereas CP exhibited optimal foam stability near neutral pH owing to favorable phosphate-species distribution and interfacial packing.

(2) Ca^{2+}/Mg^{2+} showed different ion-specific effects on collector foams. Mg^{2+} mainly induced gradual foam deterioration through electrostatic regulation and collector depletion, while Ca^{2+} caused stronger destabilization, especially for CP, due to stronger interactions with phosphate headgroups and rapid formation of calcium–collector complexes.

(3) The findings demonstrate that collector headgroup chemistry and solution composition jointly determine foam stability. These results provide fundamental guidance for selecting flotation reagents and regulating water chemistry in magnesite flotation systems.

The current investigation mainly focused on the dynamic foam behavior and interfacial responses of two representative anionic collectors under controlled solution conditions, while the direct relationship between collector foam stability and actual flotation performance was not experimentally verified. Further studies incorporating mineral particles are required to correlate collector foam characteristics with practical flotation performance, including bubble–particle attachment, particle loading, and froth mobility.

Acknowledgments

The authors acknowledge with appreciation the financial assistance provided by the National Natural Science Foundation of China (52104263), the Scientific and Technological Innovation Guidance Fund of Wuhan Institute of Technology (K2026082), the Scientific and Technological Innovation Platform Research Project of Guizhou Province (CXPTXM[2025]016), and the Central Government's Special Project for Supporting Local Science and Technology Development in Hubei Province (2025CSA015).

References

ARELLANO-PIÑA, R., DELGADILLO, J., PÉREZ-GARIBAY, R., 2017, *Effect of gas superficial velocity (Jg) and frother/collector (MIBC/X-343) reagent dosage on froth horizontal displacement and galena drainage*, Miner. Eng., 114, 8–16.

ATRAFI, A., PAWLIK, M., 2016, *Surface tension and gas dispersion properties of fatty acid solutions*, Miner. Eng., 85, 138.

BHONDAYI, C., 2020, *Flotation froth phase bubble size measurement*, Miner. Process. Extr. Metall. Rev., 43, 251.

BIMPILAS, G.M., ANASTASSAKIS, G.N., 2020, *Magnesite benefiation methods: a review*, Sustain. Extr. Process. Raw Mater., 1, 14–20.

BINKS, B.P., SHI, H., 2020, *Aqueous foams in the presence of surfactant crystals*, Langmuir, 36, 991–1002.

BOURNIVAL, G., ATA, S., JAMESON, G.J., 2017, *Bubble and froth stabilizing agents in froth flotation*, Miner. Process. Extr. Metall. Rev., 38, 366.

CHEN, G., TAO, D., 2004, *Effect of solution chemistry on flotability of magnesite and dolomite*, Int. J. Miner. Process., 74, 343–357.

CHOI, J., CHOI, S.Q., PARK, K., HAN, Y., KIM, H., 2016, *Flotation behaviour of malachite in mono-and di-valent salt solutions using sodium oleate as a collector*, Int. J. Miner. Process., 146, 38.

CRAIG, V.S.J., NINHAM, B.W., RICHARD, M.P., 1993, *The effect of electrolytes on bubble coalescence in water*, J. Phys. Chem., 97, 10192.

CUI, H., CAO, G., ZHU, S., MU, J., LIU, X., CHOU, X., 2022, *Foaming performance evaluation of frother emulsions in the slime flotation: Foamability, foam stability, and foam flow*, Colloids Surf. A, 638, 128310.

FU, Z., CHEN, P., LIU, Y., 2022, *Experimental study of the influence of inorganic salts on foam stability*, Langmuir, 38, 14607–14614.

FUKUOKA, K., TOMIKAWA, A., NAKAMURA, Y., FUJI, S., 2016, *Aqueous foams stabilized with several tens of micrometer-sized polymer particles: Effects of surface hydrophilic–hydrophobic balance on foamability and foam stability*, Chem. Lett., 45, 667–669.

GONCHARIK, I.I., VOYTENKO, A.I., MOZHEYKO, F.F., POTKINA, T.N., SHEVCHUK, V.V., 2013, *The study of quenching efficiency of three-phase foams formed in flotation of phosphate rock*, Russ. J. Appl. Chem., 86, 899–904.

JISUNG, K., LIM, J.C., 2009, *Interfacial properties of imidazoline cationic surfactant*, Korean Chem. Eng. Res., 47, 38.

KANOKKARN, P., SHIINA, T., SANTIKUNAPORN, M., CHAVADEJ, S., 2017, *Equilibrium and dynamic surface tension in relation to diffusivity and foaming properties: Effects of surfactant type and structure*, Colloids Surf. A, 524, 135–142.

KEDIR, K.A.S., SOLBAKKEN, J.S., AARRA, M.G., 2022, *Foamability and stability of anionic surfactant-anionic polymer solutions: Influence of ionic strength, polymer concentration, and molecular weight*, Colloids Surf. A, 632, 127801.

KINOSHITA, T., ISHIGAKI, Y., SHIBATA, N., 2018, *Selective recovery of Indium via continuous counter-current foam separation from sulfuric acid solutions I – application of anionic organophosphate surfactant as metal collector*, Sep. Purif. Technol., 212, 563–571.

KUME, G., GALLOTTI, M., NUNES, G., 2008, *Review on anionic/cationic surfactant mixtures*, J. Surfactants Deterg., 11, 1–11.

LAN, S., DONG, L., ZHANG, T., LIU, D., SHEN, Z., 2025, *Inorganic salt regulators eliminate the adverse effects of interfering ions on the efficient flotation enrichment of phosphate ores*, Colloids Surf. A, 725, 137676.

LE, T.T.Y., HUSSAIN, S., LIN, S.Y., 2019, *A study on the determination of the critical micelle concentration of surfactant solutions using contact angle data*, J. Mol. Liq., 294, 111582.

LI, C., ZHANG, T., JI, X., WANG, Z., SUN, S., HU, S., 2016, *Effect of Ca2+/Mg2+ on the stability of the foam system stabilized by an anionic surfactant: A molecular dynamics study*, Colloids Surf. A, 489, 423–432.

LI, E., DUAN, P., DU, Z., LI, D., CHENG, F., 2016, *Colloidal properties of octadecylamine hydrochloride and the wettability of KCl crystal surface in different saturated salt solutions*, J. Mol. Liq., 223, 107.

LIM, J., 2009, *Effect of pH on physical properties of triethanolamine-ester quaternary ammonium salt cationic surfactant system*, Appl. Chem. Eng., 20, 479.

MABROUK, M.M., HAMED, N.A., MANSOUR, F.R., 2022, *Physicochemical and electrochemical methods for determination of critical micelle concentrations of surfactants: a comprehensive review*, Monatsh. Chem., 153, 125–138.

MORENO, G.A., SILVA, M., 2021, *Foam stability of flotation frothers under dynamic and static conditions*, Sep. Purif. Technol., 274, 117822.

PENG, X., ZHANG, L., YAN, Y., LIU, Y., TIAN, X., ZHU, Y., LEI, D., WANG, Y., 2024, *Unveiling the enhancement mechanism of Fe ion for muscovite flotation: Adjustment of surface potential and agent dispersion*, Colloids Surf. A, 687, 133471.

PETKOVA, B., TCHOLAKOVA, S., CHENKOVA, M., GOLEMANOV, K., DENKOV, N., THORLEY, D., STOYANOV, S., 2020, *Foamability of aqueous solutions: Role of surfactant type and concentration*, Adv. Colloid Interface Sci., 276, 102084.

PUGH, R.J., WEISSENBORN, P., PAULSON, O., 1997, *Flotation in inorganic electrolytes; the relationship between recover of hydrophobic particles, surface tension, bubble coalescence and gas solubility*, Int. J. Miner. Process., 51, 125–138.

PUGH, R.J., RUTLAND, M.W., MANEV, E., CLAESSON, P.M., 1996, *Dodecylamine collector – pH effect on mica flotation and correlation with thin aqueous foam film and surface force measurements*, Int. J. Miner. Process., 46, 245–262.

SCHELERO, N., HEDICKE, G., LINSE, P., KLITZING, R., 2010, *Effects of counterions and co-ions on foam films stabilized by anionic dodecyl sulfate*, J. Phys. Chem. B, 114, 15525–15533.

SHU, X., MENG, Y., WAN, L., LI, G., YANG, M., JIN, W., 2014, *pH-responsive aqueous foams of oleic acid/oleate solution*, J. Dispers. Sci. Technol., 35, 293–300.

SUN, W., DAI, S., LIU, W., LI, P., DUAN, H., YU, X., 2021, *Effect of Ca(II) on anionic/cationic flotation of magnesite ore*, Miner. Eng., 163, 106778.

SUN, W., DAI, S., LIU, W., YU, L., 2017, *Study on removing impurity from magnesite ore by two step reverse flotation*, Bulg. Chem. Commun., 48, 678.

TANG, Y., GUO, J., LI, F., HE, D., YIN, X., FU, Y., LI, Z., MA, J., 2026, *Selective depression of fluorapatite by malic acid: The role of soluble calcium complexation in flotation separation from dolomite*, Miner. Eng., 249, 110630.

TANG, Y., SUN, H., YIN, W., YANG, B., CAO, S., WANG, D., KELEBEK, S., 2021, *Computational modeling of cetyl phosphate adsorption on magnesite (104) surface*, Miner. Eng., 171, 107123.

TANG, Y., YIN, W., KELEBEK, S., 2020a, *Magnesite-dolomite separation using potassium cetyl phosphate as a novel flotation collector and related surface chemistry*, Appl. Surf. Sci., 508, 145191.

TANG, Y., YIN, W., KELEBEK, S., 2020b, *Selective flotation of magnesite from calcite using potassium cetyl phosphate as a collector in the presence of sodium silicate*, Miner. Eng., 146, 106154.

WANG, H., YANG, W., YAN, X., WANG, L., WANG, Y., ZHANG, H., 2020, *Regulation of bubble size in flotation: A review*, J. Environ. Chem. Eng., 8, 104070.

WANG, K., WANG, Y., PERA-TITUS, M., 2024, *Liquid–liquid and gas–liquid dispersions in electrochemistry: concepts, applications and perspectives*, Chem. Soc. Rev., 53, 11701–11724.

WANG, L., YOON, R.H., 2009, *Effect of pH and NaCl concentration on the stability of surfactant-free foam films*, Langmuir, 25, 294–297.

WANG, S., WANG, Y., KONG, R., 2024, *Investigation of flotation bubble-particle attachment interactions influenced by monovalent cations and cationic surfactants from macro and molecular scales*, Adv. Powder Technol., 35, 104549.

WEN, Y., ZENG, P., XU, L., LI, Q., GUAN, X., WEI, K., WANG, X., 2024, *Impacts of hydrophobic chain length on foam stability and CO2 geo-sequestration capacity of sugar-based nonionic surfactants: Molecular dynamics simulation and laboratory experiments*, J. Environ. Chem. Eng., 12, 114643.

WONYEN, D.G., KROMAH, V., GIBSON, B., NAH, S., CHELGANI, S.C., 2018, *A review of flotation separation of Mg carbonates (dolomite and magnesite)*, Minerals, 8, 354.

XIE, L., SHI, C., CUI, X., ZENG, H., 2017, *Surface forces and interaction mechanisms of emulsion drops and gas bubbles in complex fluids*, Langmuir, 33, 3911–3925.

XIE, W., HE, D., LIU, S., CHEN, F., LI, H., 2020, *Effect of pH and dodecylamine concentration on the properties of dodecylamine two-phase foam*, J. Chem. Soc. Pak., 42, 495.

XING, Y., GUI, X., PAN, L., PINCHASIK, B.E., CAO, Y., LIU, J., KAPPL, M., BUTT, H.J., 2017, *Recent experimental advances for understanding bubble-particle attachment in flotation*, Adv. Colloid Interface Sci., 246, 105–132.

XING, Y., GUI, X., CAO, Y., WANG, Y., XU, M., WANG, D., LI, C., 2017, *Effect of compound collector and blending frother on froth stability and flotation performance of oxidized coal*, Powder Technol., 305, 166–173.

XU, M., GUO, F., BAO, X., GUI, X., XING, Y., CAO, Y., 2023, *Study on the strengthening mechanism of a MIBC–PEG mixed surfactant on foam stability*, ACS Omega, 8, 27429.

XU, Y., XU, L., WU, H., TIAN, J., WANG, Z., GU, X.C., 2020, *The effect of citric acid in the flotation separation of bastnaesite from fluorite and calcite using mixed collectors*, Appl. Surf. Sci., 529, 147–166.

PAN, Y., BOURNIVAL, G., ATA, S., 2022, *Effect of electrolyte and flotation collector on foam films in the presence of frothers*, Chem. Eng. Sci., 264, 118–176.

YAMANAKA, T., 1975, *Effects of electrolytes on properties of black films and foam stability of aqueous nonionic surfactant solutions*, Bull. Chem. Soc. Jpn., 48, 1760–1763.

YIN, W., LI, Q., MA, Y., 2010, *Flotation research on dolomite-containing magnesite ore*, Adv. Mater. Res., 158, 113–117.

ZAWALA, J., TODOROV, R., OLSZEWSKA, A., MALYSA, K., 2010, *Influence of pH of the BSA solutions on velocity of the rising bubbles and stability of the thin liquid films and foams*, Adsorption, 16, 423–435.

ZHANG, N., CHEN, X., PENG, Y., 2020, *Effects of froth properties on dewatering of flotation products– A critical review*, Miner. Eng., 155, 106477.

ZHANG, P., CAO, X., LI, X., GUO, D., BIAN, J., DONG, H., 2021, *Microscopic mechanisms of inorganic salts affecting the performance of aqueous foams with sodium dodecyl sulfate: View from the gas–liquid interface*, J. Mol. Liq., 343, 117488.

ZHU, W., ZHU, H., ZHU, J., ZHANG, Y., CHEN, K., MENG, Q., ZENG, Q., JI, Z., 2025, *Effect of inorganic cations on bubble-oil droplet coalescence in aqueous solution*, Colloids Surf. A, 726, 137778.